

SUPPORTING INFORMATION FOR

Chemical Composition and Morphological Analysis of Atmospheric Particles from an Intensive Bonfire Burning Festival

Jay M. Tomlin¹, Johannes Weis³, Daniel P. Veghte^{4,†}, Swarup China⁴, Matthew Fraund³, Quanfu He⁵,
Naama Reicher⁵, Chunlin Li⁵, Kevin A. Jankowski¹, Felipe A. Rivera-Adorno¹, Ana C. Morales,¹ Yinon
Rudich⁵, Ryan C. Moffet⁶, Mary K. Gilles³, Alexander Laskin^{1,2*}

¹Department of Chemistry, ²Department of Earth Atmospheric and Planetary Sciences, Purdue University, West
Lafayette, IN 47907, USA

³Chemical Sciences Division, Lawrence Berkeley National Laboratory, Berkeley, CA 94720, USA

⁴Environmental Molecular Sciences Laboratory, Pacific Northwest National Laboratory, Richland, WA 99354, USA

⁵Department of Earth and Planetary Sciences, Weizmann Institute of Science, Rehovot 76100, Israel

⁶Sonoma Technology, Inc., Petaluma, CA 94954, USA

†Current address: Center for Electron Microscopy and Analysis, Ohio State University, Columbus, OH 43212, USA

Correspondence to: Alexander Laskin (alaskin@purdue.edu)

TABLE OF CONTENTS

Figure S1	3
Figure S2	3
Figure S3	4
Table S1	4
Figure S4	5
Figure S5	5
Figure S6	7
Figure S7	8
Figure S8	9
Figure S9	10
Figure S10	11

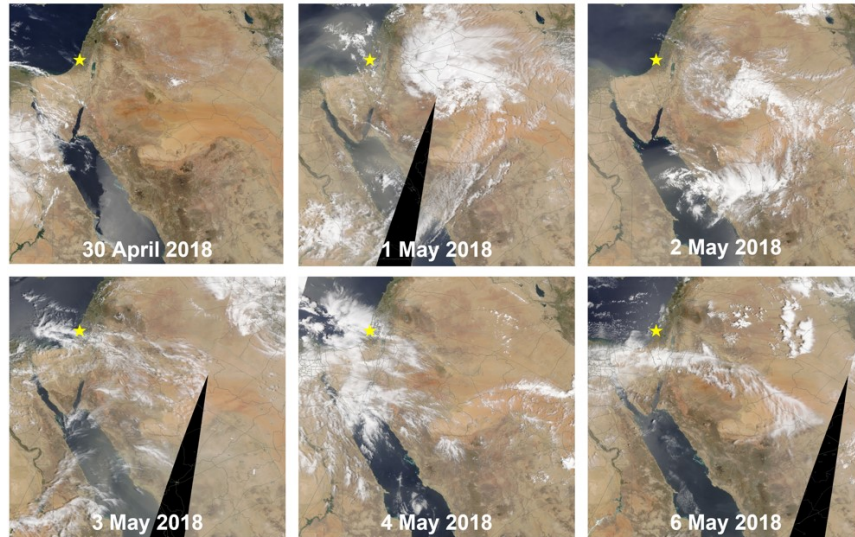


Figure S1. MODIS corrected reflectance satellite images of Southwest Asia visualized from NASA Worldview and Global Imagery Browse Services (GIBS) at 250 m resolution.¹ The marker corresponds to the location of sampling site in Rehovot, Israel. Image progression shows the approaching dust storms from the Arabian Desert (eastern) and Sahara Desert (western). The preceding dust plumes appear to settle in the region days after the initial dust storm event.

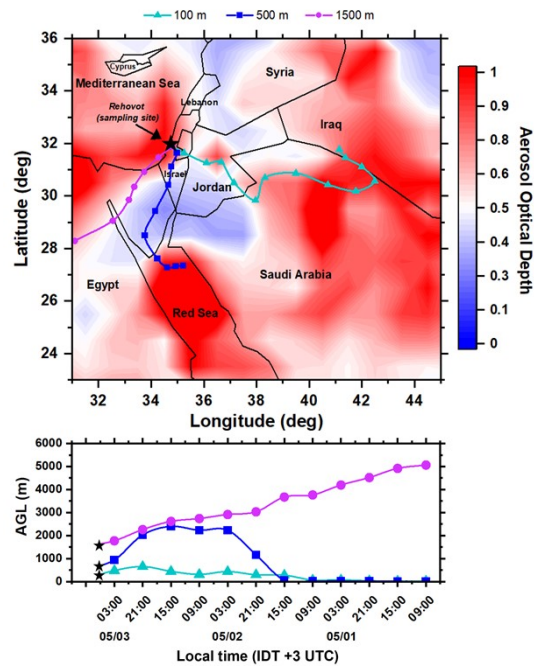


Figure S2. Combined MODIS Terra and Aqua sensor at $1^\circ \times 1^\circ$ daily average aerosol optical depth (AOD) from 1 May to 4 May 2018. Samples were collected between morning of 2 May and afternoon of 3 May 2018. AOD map shows large aerosol plumes around the surrounding regions including Arabian Desert, Sahara Desert, Mediterranean Sea, and Red Sea. The black marker shows the location of the sampling site (Rehovot, Israel). Colored lines indicate the 72 hr HYSPLIT back trajectory ending at the sampling site during peak of the burning event at different starting elevations: 100 m (teal), 500 m (blue), 1500 m (pink). Markers on the trajectories denote position of the air parcel at 6 hr intervals between 01:00 IDT 4 May to

09:00 IDT (+3 UTC) 30 April 2018 while time series below shows the location of the parcels calculated from HYSPLIT.^{2,3}

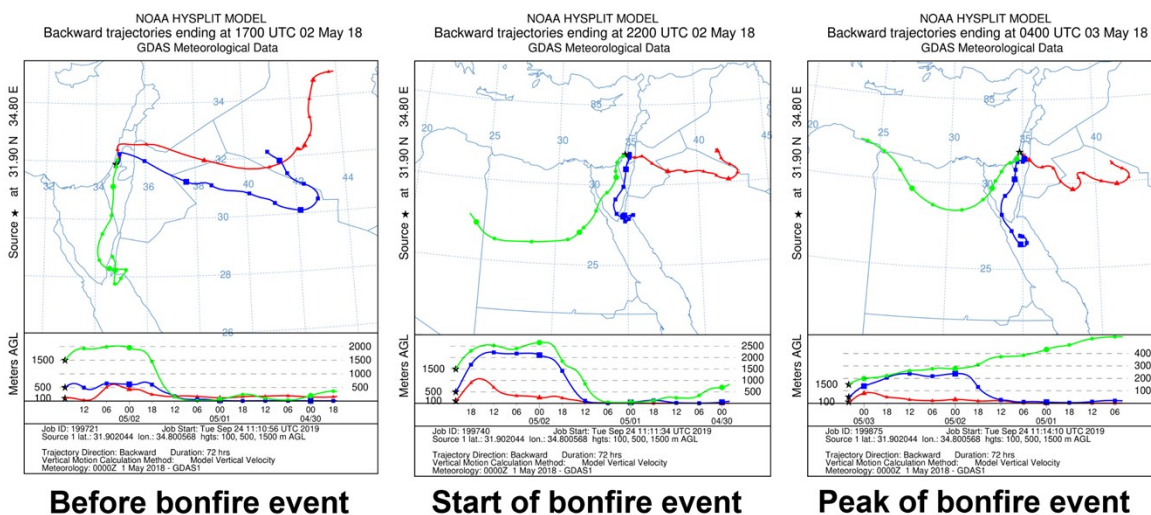


Figure S3. Hybrid Single-Particle Lagrangian Integrated Trajectory (HYSPLIT)^{2,3} back trajectories for dry intrusion periods utilizing global data assimilation system (GDAS1) model data at three starting elevations 100 m (red), 500 m (blue), 1500 m (green) calculated for the different sampling time periods. The synoptic conditions were found to be Sharav low, which are tropical depressions typically formed over North Africa. These events are characterized by hot and dry conditions accompanied by frequent dust storms. Air masses are initially transported from the Arabian (eastern) and then from the Sahara (western) desert.

Table S1. MOUDI particle sampling information

Sample no.	Date (2018)	Sampling period (IDT, +3 UTC)	No. of particles analyzed with CCSEM	No. of particles analyzed with STXM	Conditions	Burning phase
1	2 May	Day 14:38–15:20	2621/2447	755	Background (pre-bonfire)	n/a
1	2 May	Day 17:05–18:05			Background (continued)	n/a
2	2 May	Night 22:50–23:50	1490/1236	314	Bonfire event (small peak)	Open fire
3	3 May	Night 03:08–03:38	1408/1622	386	Bonfire event (peak)	Mixed open fire/smoldering
4	3 May	Day 06:05–06:25	3543/3048	266	After sunrise	Smoldering
5	3 May	Day 09:28–09:40	4135/1630	267	Morning	Smoldering
6	3 May	Day 11:56–12:54	1751/1641	152	Noon	Smoldering

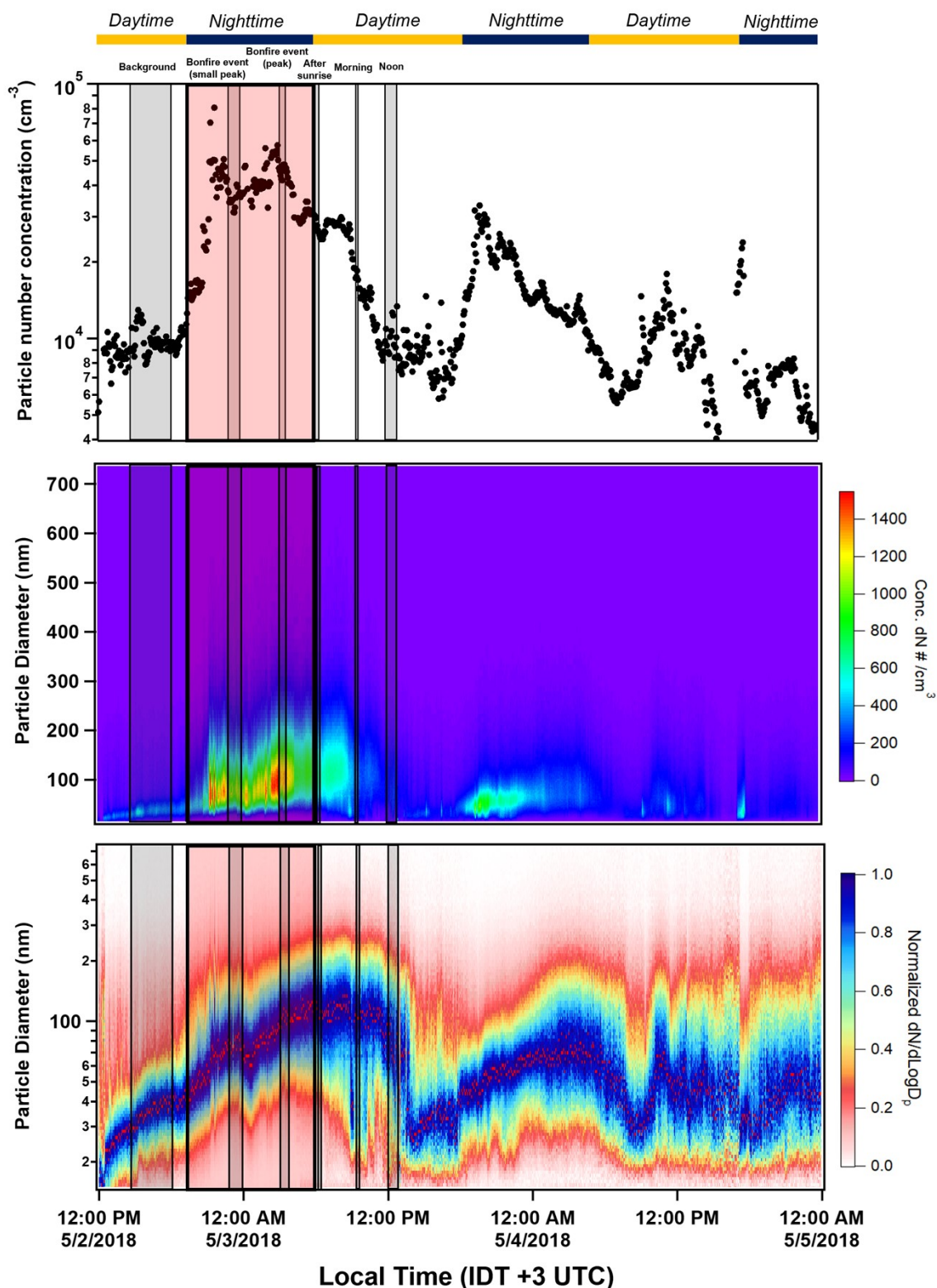


Figure S4. SMPS number concentration, mobility size distribution, and mobility size distribution normalized to the maximum concentration between 12:00 IDT 2 May 2018 to 00:00 5 May 2018. The grey shaded regions corresponding to the MOUDI sampling time periods while the red shaded region shows the official time of the Lag Ba’Omer bonfire festival (19:22 IDT 2 May 2018 to 05:54 IDT 3 May 2018). The daytime (yellow line) and nighttime (dark blue line) cycle is also shown above.

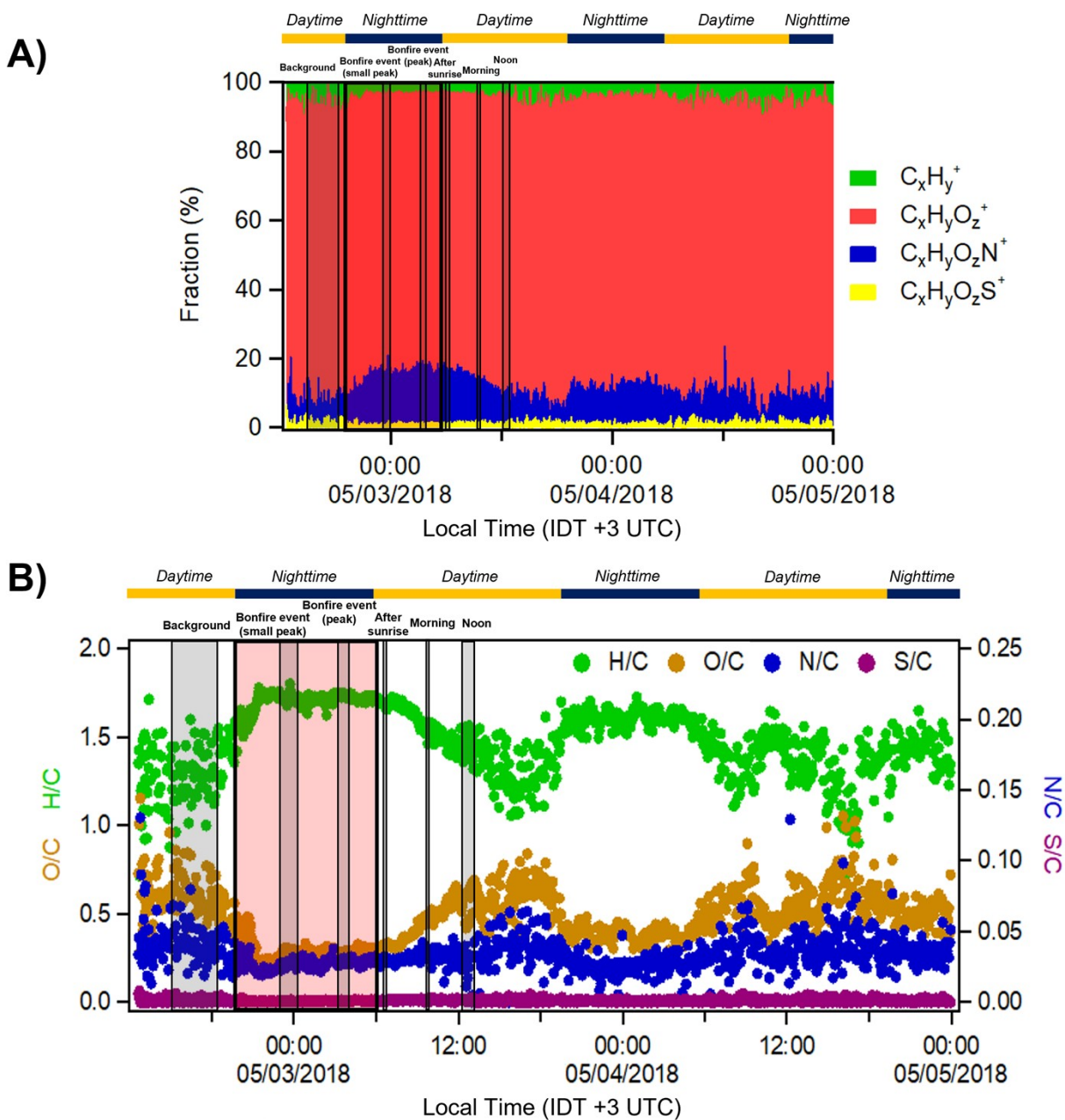


Figure S5. (A) Time series of the relative contribution of different fragments groups to organic aerosols identified from AMS measurements. (B) Elemental composition of organic aerosols measured during the event and following days after the burning period. The grey shaded regions corresponding to the MOUDI sampling time periods while the red shaded region shows the official time of the Lag Ba’Omer bonfire festival (19:22 IDT 2 May 2018 to 05:54 IDT 3 May 2018). The daytime (yellow line) and nighttime (dark blue line) cycle is also shown above.

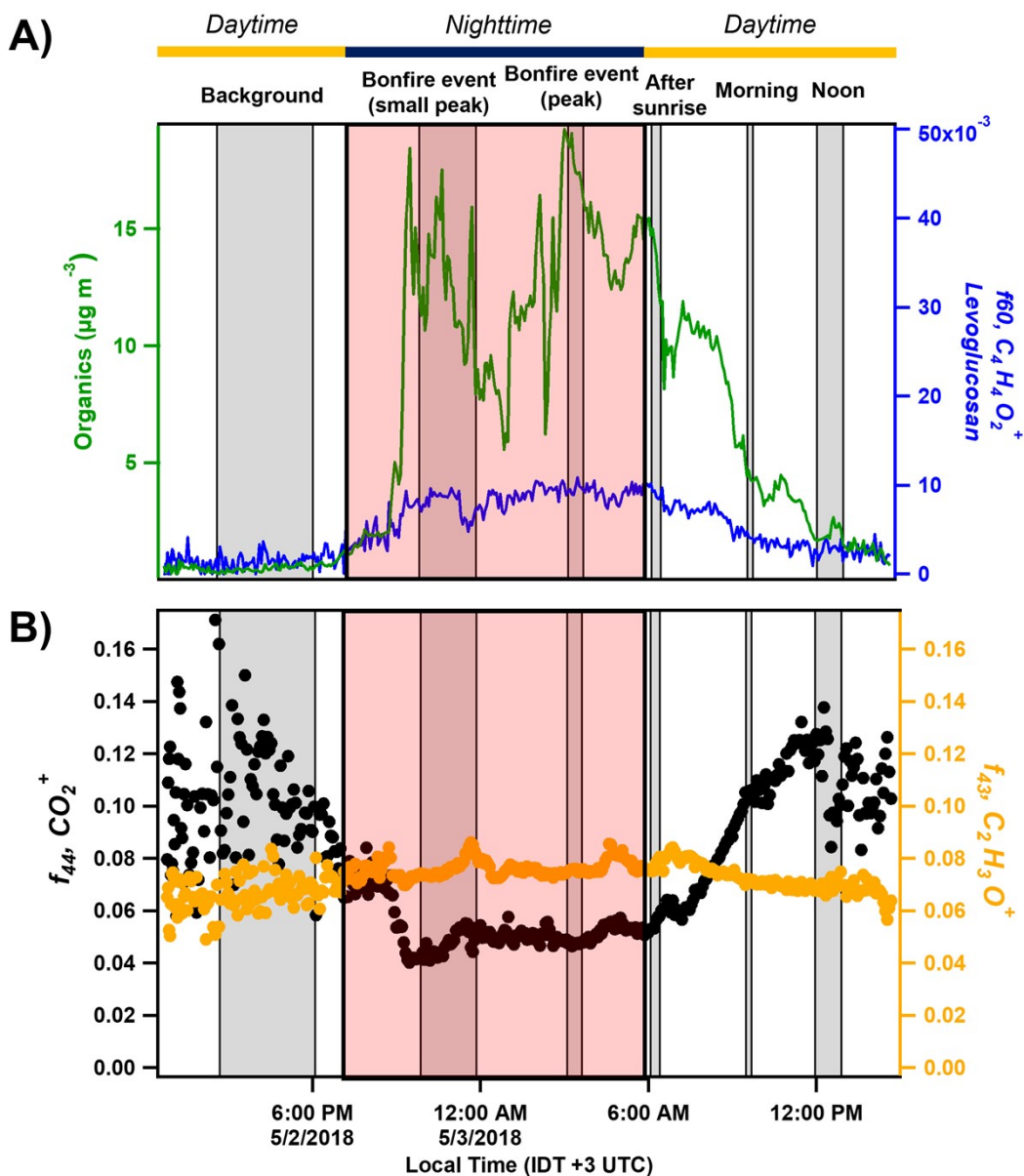


Figure S6. (A) Total organic mass concentration and f_{60} (i.e., mass fragment for levoglucosan) quantified by AMS. The f_{60} dataset were anchored to match the background levels of the total organic mass concentration. (B) Time series of f_{43} and f_{44} within the relevant burning period. The grey shaded regions corresponding to the MOUDI sampling time periods while the red shaded region shows the official time of the Lag Ba'Omer bonfire festival (19:22 IDT 2 May 2018 to 05:54 IDT 3 May 2018). The daytime (yellow line) and nighttime (dark blue line) cycle is also shown above.

Estimating effective particle density

The effective particle density (ρ_{eff}) of ambient particle during the burning event and the following days were estimated by comparing the aerodynamic diameters (D_{ae}) recorded by an Aerodynamic Aerosol Classifier (AAC) to the mode mobility diameter (D_{m}) obtained from SMPS at discrete aerodynamic sizes of 100/150/200/250/300 nm using the following relationship assuming a 1.0 g/cm^3 unit density (ρ_0),⁴

$$\rho_{\text{eff}} = \frac{D_{\text{ae}}}{D_{\text{m}}} \rho_0 \quad (1)$$

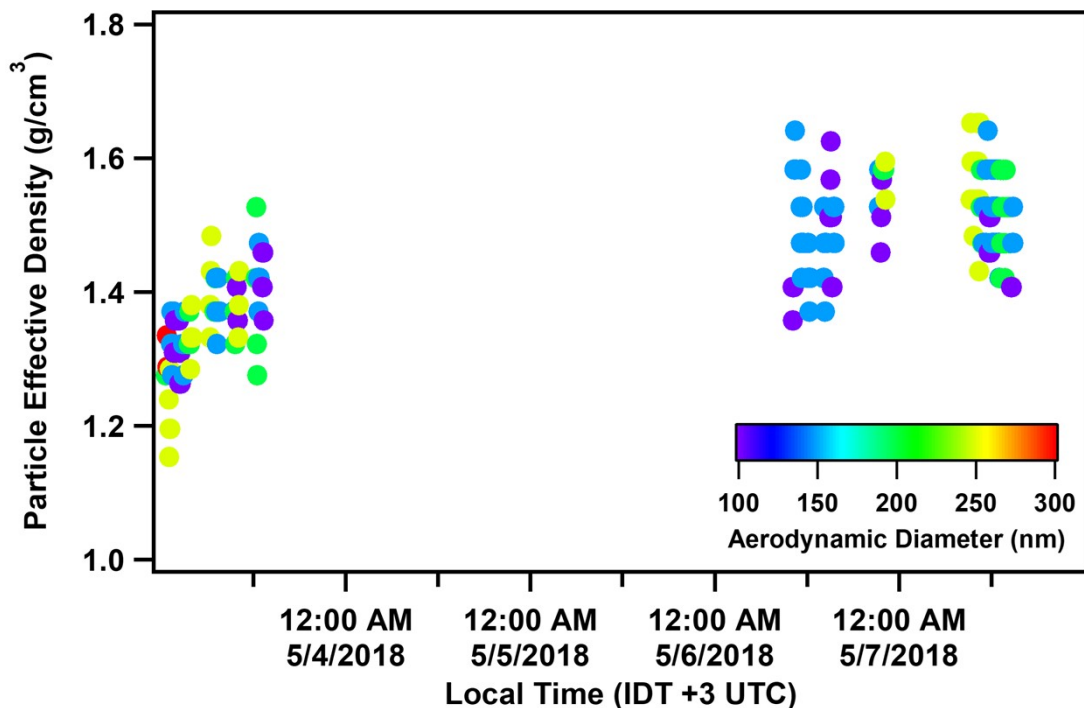


Figure S7. Particle effective density as a function of time and aerodynamic diameter within the peak burning period (00:00 3 May 2018 to 13:00 3 May 2018) and a few days after (6 and 7 May 2018).

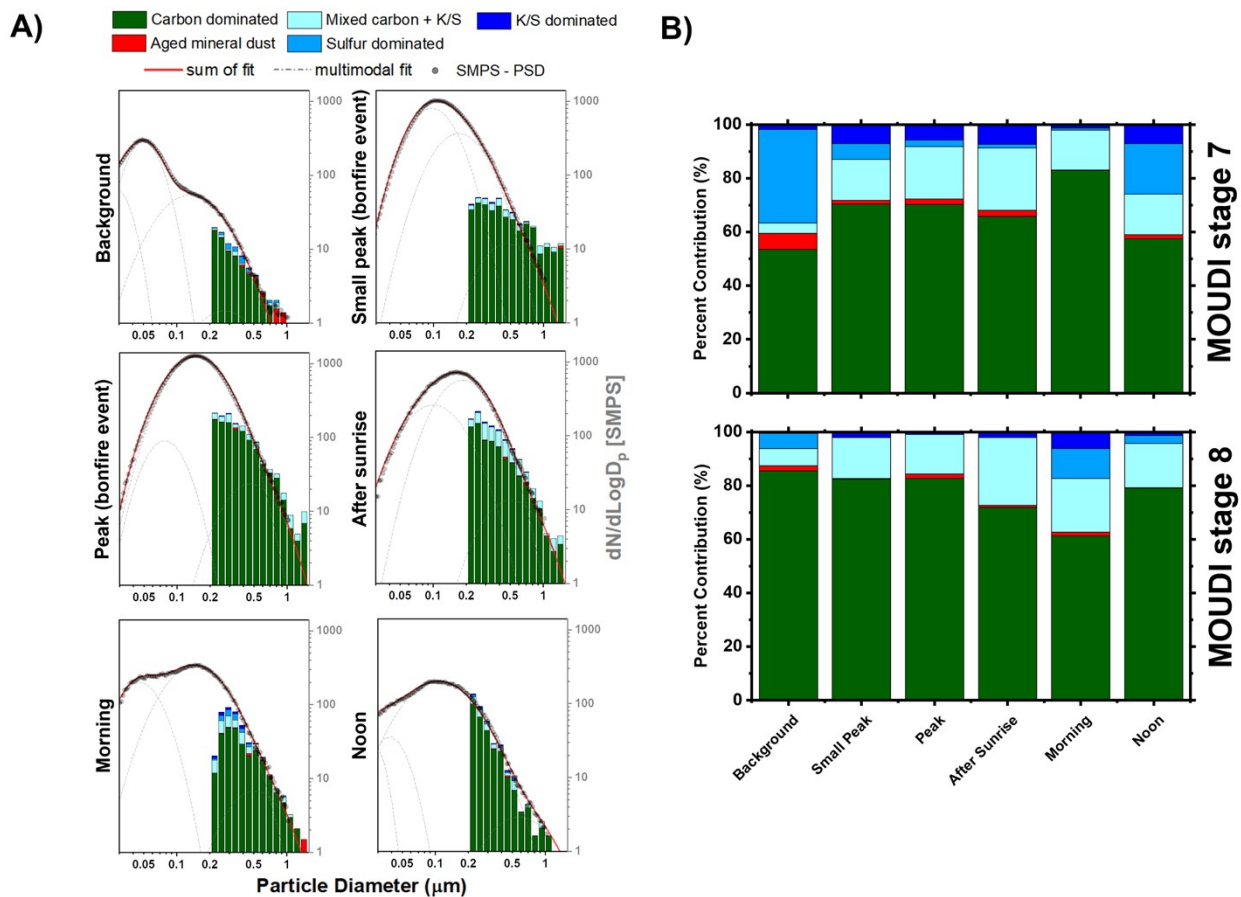


Figure S8. (A) MOUDI stage 8: size resolved particle-type classification obtained from CCSEM/EDX and identified by *k*-means clustering analysis plotted as a 16 bin/decade histogram in logscale for different sampling periods of the wood burning event. The SMPS aerosol size distribution measured during the same time periods were superimposed and anchored at 0.50 μm to facilitate a visual comparison. Lognormal fits were applied to the SMPS particle size distribution measurements. Grey dashed line corresponds to the individual modal fit while the red solid line is the sum of the fits. (B) Percent contribution of particle-types identified by the algorithm for different periods of the wood burning event; Top – MOUDI stage 7; Bottom – MOUDI stage 8.

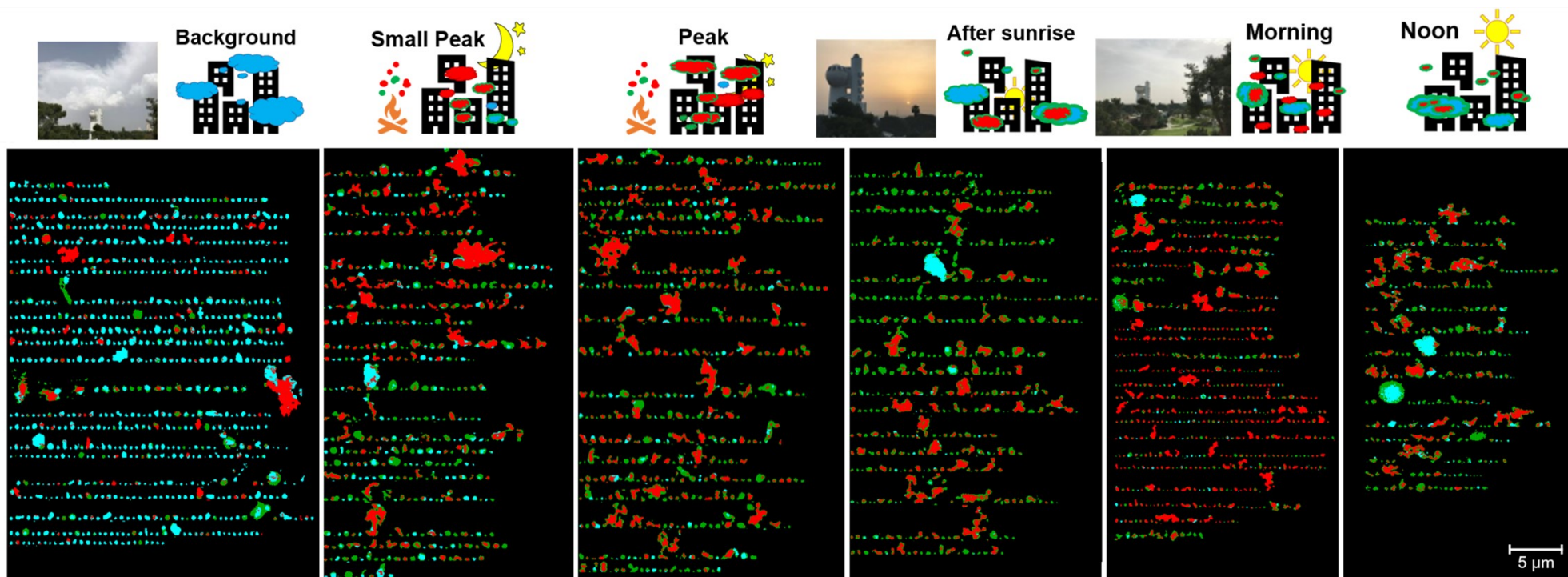


Figure S9. Compilation of carbon speciation maps based on STXM/NEXAFS measurements for different sampling periods. Regions dominated by organics are shown in green, inorganic dominated areas are teal, and soot/elemental carbon are mapped as red. Note that components can overlap resulting in mixed colors. The illustrations and picture above show the different periods of the wood burning event and the accumulation different aerosol types with the progression of particle mixing state in the urban region denoted by the colored plumes. Note that STXM measures the absorption through the particle, and therefore, each pixel can contain up to three components (i.e., EC, IN, and OC regions may overlap).

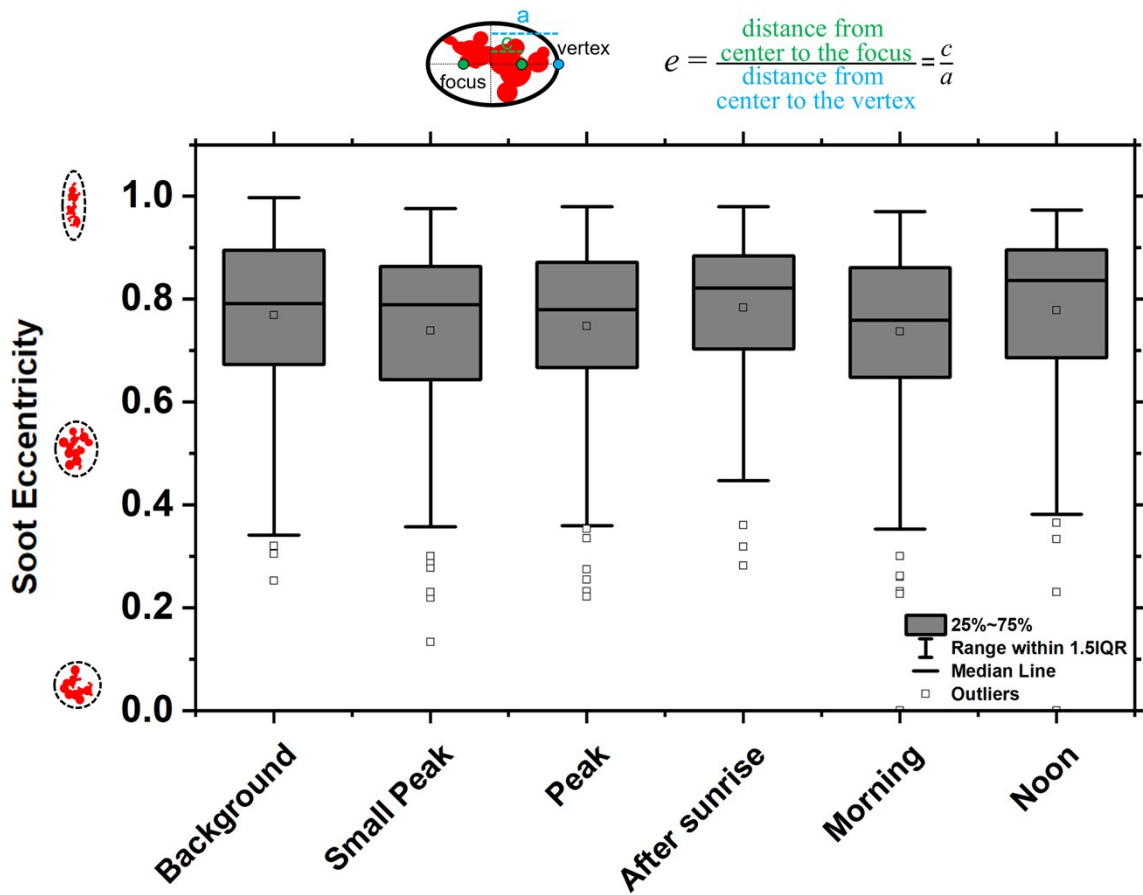


Figure S10. Box and whisker plot of soot inclusion eccentricity across different sampling. Eccentricity is obtained by applying a best fit ellipse around a soot inclusion and calculating the ratio of the length of the c (i.e., distance from center to the focus) to the length of a (i.e., distance from center to the vertex), as shown in the illustration above.

References

- 1 MODIS Characterization Support Team (MCST), 2017. MODIS 250m Calibrated Radiances Product. NASA MODIS Adaptive Processing System, Goddard Space Flight Center, USA.
- 2 A. F. Stein, R. R. Draxler, G. D. Rolph, B. J. B. Stunder, M. D. Cohen and F. Ngan, *Bull. Am. Meteorol. Soc.*, 2015, **96**, 2059–2077.
- 3 G. Rolph, A. Stein and B. Stunder, *Environ. Model. Softw.*, 2017, **95**, 210–228.
- 4 C. Li, Q. He, J. Schade, J. Passig, R. Zimmermann, D. Meidan, A. Laskin and Y. Rudich, *Atmospheric Chem. Phys.*, 2019, **19**, 139–163.